



Evaluating the potential of natural polymers for water-dispersible curcumin-based solid dispersion colourant systems for food applications

Stephany Cunha de Rezende^{a,b,c,d}, Olga Ferreira^{a,b}, Arantzazu Santamaria-Echart^{a,b,**},
Madalena Maria Dias^{c,d}, Maria Filomena Barreiro^{a,b,*}

^a Centro de Investigação de Montanha (CIMO), Instituto Politécnico de Bragança, Campus de Santa Apolónia, 5300-253, Bragança, Portugal

^b Laboratório Associado para a Sustentabilidade e Tecnologia em Regiões de Montanha (LA SusTEC), Instituto Politécnico de Bragança, Campus de Santa Apolónia, 5300-253, Bragança, Portugal

^c Laboratory of Separation and Reaction Engineering – Laboratory of Catalysis and Materials (LSRE-LCM), Department of Chemical Engineering, Faculty of Engineering University of Porto, Rua Dr. Roberto Frias, 4200-465, Porto, Portugal

^d Associate Laboratory in Chemical Engineering (ALiCE), Faculdade de Engenharia, Universidade do Porto, R. Dr. Roberto Frias, 4200-465, Porto, Portugal

ARTICLE INFO

Keywords:

Solid dispersions
Natural food colourants
Curcumin
Natural polymers
Water solubility

ABSTRACT

Solid dispersion (SD) technology, a strategy through which a hydrophobic compound is molecularly dispersed into a hydrophilic carrier, is raising interest in food applications to surpass natural colourants' low water solubility. Motivated by the importance of using natural solutions, five natural polymers (k-carrageenan (KC), maltodextrin (MD), Arabic gum (AG), potato starch (PS), and pectin (PC) were evaluated against the synthetic benchmark polyvinylpyrrolidone (PVP)). Targeting a stable yellow hue, pH 6 was used, and the effect of salt addition on crystallinity was evaluated. Comparatively with PVP, used as a synthetic polymer reference, SDs based on MD, AG, and PC presented a deeper orange shade. Similar size distributions were achieved for the produced samples except for PS-based SDs, which showed higher sizes in volume. For all systems, polymer-curcumin hydrogen bonding was perceptible and reflected in the curcumin crystallinity modification/reduction, particularly if produced under natural pH conditions. The water solubility was significantly improved compared to free curcumin, from 1 µg/mL to 25–37 µg/mL (pH 6, PVP - 24.54 µg/mL) and 18–86 µg/mL (without pH control, PVP - 28.34 µg/mL), highlighting the favourable effect of natural polymers.

1. Introduction

With the restrictions imposed on synthetic colourant applications, the food industry urges natural and less toxic alternatives (Fernández-López et al., 2020). This assumes a particular relevance for the red and yellow shades, representing approximately 90 % of the colourants added to food (Gordillo et al., 2018). Nevertheless, the application of available natural counterparts, mostly carotenoids, is usually limited, considering their stability and poor water solubility.

Several approaches have been proposed to circumvent carotenoids' water compatibility constraints (Boer et al., 2019; Santos and Meireles, 2010), most of them based on encapsulation processes. Some of the reported strategies encompass the preparation of astaxanthin-loaded oil-in-water emulsions (Mezquita et al., 2020), β-carotene

encapsulation in soluble complexes formed by whey protein and OSA-modified starch (Lin et al., 2021), bixin encapsulation in particles of modified starch and gelatin blends (Balakrishnan et al., 2021), carotenoid-rich extracts encapsulation in porcine gelatin, whey protein isolate and concentrate (Medeiros et al., 2019), and β-carotene-loaded oleogel-in-water Pickering emulsions (Qi et al., 2020). Most of the studied strategies targeted the enhancement of oral bioavailability, which depends on water compatibility, with few addressing water-solubility determination. Among the cited examples, it was possible to achieve a solubility of circa 264 µg/mL for β-carotene (Lin et al., 2021) and 72 µg/mL for carotenoid-rich extracts from Cantaloupe melon (Medeiros et al., 2019).

Alternative approaches to enhance the water compatibility of carotenoids are based on solid dispersions (SDs). SD technology can be

* Corresponding author. Centro de Investigação de Montanha (CIMO), Instituto Politécnico de Bragança, Campus de Santa Apolónia, 5300-253, Bragança, Portugal.

** Corresponding author. Centro de Investigação de Montanha (CIMO), Instituto Politécnico de Bragança, Campus de Santa Apolónia, 5300-253, Bragança, Portugal.

E-mail addresses: asantamaria@ipb.pt (A. Santamaria-Echart), barreiro@ipb.pt (M.F. Barreiro).

<https://doi.org/10.1016/j.jfoodeng.2024.111986>

Received 3 September 2023; Received in revised form 20 January 2024; Accepted 24 January 2024

Available online 31 January 2024

0260-8774/© 2024 The Authors. Published by Elsevier Ltd. This is an open access article under the CC BY-NC-ND license (<http://creativecommons.org/licenses/by-nc-nd/4.0/>).

defined as the dispersion of an active compound (usually hydrophobic and crystalline) in a solid matrix (e.g., a hydrophilic polymeric matrix), favoring amorphisation, and thus improving the water compatibility and dissolution rate (Pandi et al., 2020). They can be produced using different methods, e.g., melt/fusion, melting solvent, and solvent evaporation. Among them, the solvent evaporation technique, which is mostly applied with carotenoids, involves the dissolution and mixture of the two components (polymer and active principle) in a common solvent or in two miscible solvents (water and ethanol) when of incompatible nature, followed by a drying stage (Li et al., 2015) through conventional oven drying, spray-drying, or freeze-drying (Lan et al., 2019; Umemoto et al., 2020). Among the drying techniques, freeze-drying can offer advantages for thermolabile products (Tran et al., 2019; Vo et al., 2013). In general, the use of SDs provides the potential to significantly enhance the solubility of hydrophobic compounds, ranging from 2 to 400 times (Khan et al., 2022).

SDs are widely applied in the pharmaceutical area, with the produced systems mostly based on synthetic polymers (e.g., PVP) and commercial pharmaceutical carriers (e.g., Eudragit® and Soluplus®). Examples include the development of β -carotene based SDs using polyvinylpyrrolidone (PVP) and sucrose fatty esters (Ishimoto et al., 2019; Otani et al., 2020). SDs of lutein and lycopene were also produced using PVP and Gelucire 44/14 (Faisal et al., 2013; Sato et al., 2018). Pursuing the interest of final consumers for natural label products, SDs are evolving to natural-based polymer formulations. Natural polymers, such as maltodextrin (MD) and Arabic gum (AG), have been studied to mitigate the flavour of pea protein or to improve the oral bioavailability of encapsulated artemisin (Lan et al., 2019; Meliana et al., 2020). Starch and pectin (PC) were also tested to protect albendazole and vitamin C, revealing the high potential for SDs (Christina et al., 2015; Nadaf et al., 2021).

Curcumin, known for its remarkable pharmacological properties, was studied using several Eudragit® type carriers and synthetic polymers (Meng et al., 2015; Zong et al., 2022). Reported solubility values can range from 64 to 900 $\mu\text{g}/\text{mL}$, dependent on the used polymer, polymer/curcumin ratio (a higher ratio favours solubility) and testing solubilization conditions (a higher temperature favours solubility), among others (Nogami et al., 2021; Wan et al., 2012). Considering natural polymers, only a few works focus on curcumin-SDs, with approaches involving the preparation of polymer blends to form protective shells around SD particles. This is the case of Arabic and xanthan gums that were used as shell material for curcumin-ethyl cellulose SDs to enhance curcumin intestinal absorption (Pinlaor et al., 2021), and PC combined with tannic acid to coat curcumin loaded micelles self-assembled from disodium glycyrrhizin (Na_2GA), to develop a core-shell SD to improve curcumin oral bioavailability (Zhang et al., 2021).

In a recent work which proposes the development of curcumin natural-based food colouring systems, SDs were produced with k-carrageenan (KC) (Leimann et al., 2019). Apart from the expected water dispersibility increase (not determined experimentally), the authors also reported that the stability against determinant factors in food processing, e.g., pH and temperature, was improved by applying SDs. Also, this work disclosed the important role of pH in the SDs production process, impacting water dispersibility and colour attributes. In fact, the pH modifies the ionisation state of the compounds, leading to different levels of hydrogen bonding between the hydrophilic polymer and the hydrophobic active compound. Therefore, maintaining the appropriate pH conditions is essential for optimising SDs formation, stability, and performance. In particular, SDs produced at pH 6 were reported to present a deep yellow hue and good colour stability.

In this work, a comparative study of five natural polymers KC, MD, AG, potato starch (PS), and PC with a synthetic polymer (PVP) was performed, aiming at understanding their suitability to develop water-dispersible curcumin-based natural colourant systems based on SDs produced by the solvent evaporation technique. The effect of using different natural polymers on colour, particle size, hydrogen bonding

(Fourier-transform infrared spectroscopy, FTIR), thermal properties (differential scanning calorimetry, DSC), crystallinity (X-ray diffraction, XRD), and water solubility of curcumin-based SDs were determined against a reference SD based on the synthetic polymer, PVP. To inspect the impacts of salt addition (associated with the pH adjustment) and curcumin molecular dispersion in the polymer (associated with SDs formation) on crystallinity and water solubility, samples without salts and physical mixtures (PMs) mimicking SDs formulations were analysed. Moreover, understanding SDs formation mechanism and their impact on particle properties is highly relevant to obtaining effective water-dispersible products, e.g., colourants for food applications.

2. Materials and methods

2.1. Materials

Curcumin (65 % purity) and the synthetic polymer PVP (PVP40, molecular weight of $40,000 \text{ g mol}^{-1}$) were acquired from Sigma-Aldrich (Saint Louis, MO, USA). As natural polymers, KC, obtained from Acros Organics (Geel, Belgium), MD (dextrose equivalent of 18), kindly donated by Cargill (Wayzata, MN, USA), AG from acacia, provided from Fisher Scientific UK (Loughborough, England), PS, purchased from Panreac Quimica S.L.U (Barcelona, Spain) and PC from the citrus peel (galacturonic acid of 74 %), obtained from Sigma Aldrich (Saint Louis, MO, USA) were used. The emulsifier polysorbate 80 (Tween 80) was provided by Panreac Quimica S.L.U (Barcelona, Spain). The buffer solutions were prepared with citric acid (99.0 %), obtained from Merck Millipore (Darmstadt, Germany), and sodium citrate (99.0 %) from Panreac Quimica S.L.U (Barcelona, Spain). Absolute ethanol (99.8 %) and methanol (99.8 %) were purchased from Honeywell (Seelze, Germany).

2.2. SDs preparation

The procedure, based on the solvent evaporation method, and formulation were adapted from the group's previous work with minor modifications. It corresponds to the formulation giving rise to the best colour stability with curcumin-PVP SD in a study targeting the effect of pH and heating conditions (Leimann et al., 2019). Moreover, it corresponds to a strong yellow hue, which is interesting for the targeting application, food colourant systems, which are urging natural solutions in the red and yellow hues.

Briefly, the selected polymer (0.4 g) and the surfactant Tween 80 (15 % w/w, polymer-basis, 0.06 g), used to improve SDs stability avoiding curcumin recrystallisation, were dissolved in 100 mL of citric acid/sodium citrate aqueous buffer solution (pH 6), whereas curcumin (15 % w/w, polymer-basis, 0.06 g) was dissolved in 50 mL of ethanol. After that, the aqueous solution was poured into the ethanolic one. The mixture was sonicated (Qsonica model Q500, 500 W, Newtown, CT, USA) at 70 % amplitude and 14 kHz frequency for 10 min (30 s on and 10 s off). After sonication, the mixture was submitted to a solvent evaporation step to remove the ethanol using a vacuum rotary evaporator (Büchi R-114, rotary evaporator, Flawil, Switzerland) at 40°C and 175 mbar. After the ethanol evaporation from the mixture, the samples were frozen in a freezer (LG, model GSL325PVCV, Amstelveen, Netherlands) at -20°C then dried in a freeze-dryer at -106°C to remove the water (CoolSafe 110-4, Scanvac, Vassingerød, Lyngø, Denmark). The dried samples were stored in a desiccator to avoid moisture uptake, protected from light until further characterisation. Reference formulations were produced without pH control to evaluate the effect of buffer (salts) addition (used to control the pH) on curcumin crystallinity and water solubility. Table 1 summarises the prepared formulations and respective codes. In addition, the pH of the aqueous phase for the samples prepared without pH control is presented.

Table 1

Codification of SDs reflecting the selected polymer and used pH conditions (with pH control (pH = 6) and without pH control (natural pH)).

| Polymer | With pH control | Without pH control | |
|----------------------|-----------------|--------------------|-------------|
| Polyvinylpyrrolidone | CPVP-pH | CPVP-Ref | 4.09 ± 0.04 |
| K-carrageenan | CKC-pH | CKC-Ref | 6.18 ± 0.04 |
| Maltodextrin | CMD-pH | CMD-Ref | 4.75 ± 0.02 |
| Arabic gum | CAG-pH | CAG-Ref | 4.52 ± 0.04 |
| Potato starch | CPS-pH | CPS-Ref | 4.56 ± 0.01 |
| Pectin | CPC-pH | CPC-Ref | 3.17 ± 0.04 |

*The pH values are expressed as average ± standard deviation of 3 independent measurements.

2.3. SDs characterisation

In order to compare the impact of using different natural polymers towards a synthetic benchmark on colour, the particles' colour parameters were determined using a colourimeter Konica Minolta Sensing Inc. CR-400 model (Sakai-ku, Japan). The measurements (L^* , a^* , and b^* (CIELAB space)) were performed in triplicate, and the results were expressed as average ± standard deviation. RGB colour was generated using a free online converter ("Convert EasyRGB," n.d.).

ΔE values were calculated according to Equation (1):

$$\Delta E = \sqrt{(\Delta L^*)^2 + (\Delta a^*)^2 + (\Delta b^*)^2} \quad (1)$$

where ΔL^* , Δa^* , and Δb^* represent the differences between the colour parameters of the SD and the control (the system using the polymer PVP (CPVP-pH, reference)).

The particle size distributions were obtained by laser diffraction using a DLS Mastersizer 3000 equipped with a Hydro MV unit, Malvern Instruments (Worcestershire, United Kingdom). Results were determined by averaging 5 consecutive measurements for each sample at room temperature using distilled water as the dispersant medium. The distributions in number and volume were obtained. The average size was determined as the Brouckere mean diameter ($d_{4,3}$), which reflects the size of those particles constituting the bulk of the sample volume. In addition, the distribution width was quantified by the span, a polydispersity indicator related to the amplitude of the 10 and 90 % of the sample relative to the central point. The lower the value, the more uniform the size distribution.

To analyse polymer-curcumin hydrogen bonding development, the FTIR spectra were acquired using an MB300 FTIR from ABB (Zurich, Switzerland) operating in attenuated total reflectance (ATR) mode using an ATR cell equipped with a diamond crystal. The spectra were obtained in the 4000 and 550 cm^{-1} range by averaging 32 scans min^{-1} at a resolution of 4 cm^{-1} . The data were acquired and treated using the Horizon MB v.3.4 software.

DSC characterisation was carried out using a DSC 204 F1 Phoenix equipment of Netzsch to evaluate the changes in melting temperature associated with curcumin crystalline modifications when incorporated in SDs. For that, 5–10 mg of the sample was sealed in aluminium pans and subjected to a heating scan from –75 to 200 °C using a heating rate of 10 °C min^{-1} under an N_2 atmosphere.

To verify the amorphisation of the curcumin crystalline structure in SDs, powder XRD analysis was carried out using the powdered samples in a conventional Bragg–Brentano diffractometer (Bruker D8 Advance DaVinci, Germany) equipped with $\text{CuK}\alpha$ radiation under 40 kV and 40 mA. Diffractograms were collected between 10 and 60° diffraction angles (2theta) with a step size of 0.05° and 1s per step.

2.4. Water solubility tests

To rationalize the effect of using different natural polymers and the effect of pH adjustment on water solubility, tests were carried out following methodologies previously described in the literature by (Mai

et al., 2020; Nogami et al., 2021), with minor modifications. Briefly, the samples were weighted and dispersed in distilled water (7 mL in a concentration of approximately 0.5 mg curcumin/mL water), to obtain saturated solutions. The samples were disposed in conical-bottom glass tubes and shaken continuously at 300 rpm at 25 °C in a thermomixer (ThermoMixer® C, Eppendorf, Hamburg, Germany) for 24 h. After shaken, the samples were centrifuged (Centrifuge 5810 R, Eppendorf, Hamburg, Germany) at 25 °C and 1500 rpm for 20 min. Samples of about 2 mL were collected from the supernatant and filtered using a 0.45 μm polytetrafluoroethylene syringe filter and then diluted with MeOH 50 % (v/v) to obtain a suitable concentration within the calibration range. Curcumin quantification was performed by UV–VIS spectroscopy (UV-VIS Spectrophotometer, Jasco V-730, Tokyo, Japan) at 420 nm. At this wavelength, all the used polymers showed no interference. A calibration curve in the curcumin concentration range of 1–10 $\mu\text{g}/\text{mL}$ ($y = 128409x - 0.0088$, $R^2 = 0.9964$) was prepared using MeOH 50 % (v/v) as the solvent. Samples were collected after the shaking step at 2 and 24 h. Solubility equilibrium is expected to be achieved in 2 h, while 24 h was used to check the solubility maintenance. All the samples were evaluated in triplicate, and the results were expressed as the average ± standard deviation. For comparison purposes, the solubility of curcumin was also assessed.

2.5. Statistical analysis

The water solubility results were analysed using ANOVA and Tukey and Student's tests ($\alpha = 0.05$), performed in Statistica StatSoft Inc. (2011) (version 10, Tulsa, OK, USA). Tukey's test was employed to determine statistically significant differences between the means of three or more groups, whereas Student's test was utilised for comparing the means of two independent groups.

3. Results and discussion

3.1. SDs colour determination

The colour parameters (L^* , a^* and b^*), and ΔE (calculated against CPVP-pH, the referenced formulation using the synthetic polymer PVP), and the RGB colour for the SD samples prepared with pH control (pH = 6) are presented in Table 2. Although the formulations contained the same curcumin amount, they evidenced different hues in the yellow-orange range, mainly dependent on a^* parameter. The CMD-pH, CAG-pH, CPS-pH and CPC-pH samples showed higher a^* values associated with a higher red colour contribution. These formulations presented a deeper colour (intense orange), comparatively with the others (CPVP-pH and CKC-pH). Additionally, in the CKC-pH and CPS-pH, ΔE values were lower than those of the other samples. The CMD-pH, CAG-pH and CPC-pH samples revealed similar differences from the CPVP-pH one. In reference to PVP, according to the international perception scale (Karma, 2020) used to compare colours, all the samples fit the attribute "colours more similar than opposite". Considering that the same production process and ingredient amounts were used for all the tested formulations, the visual differences can be associated with the nature of the used polymer, which can originate distinct polymer-curcumin molecular interactions and thus influence curcumin crystallinity.

3.2. SDs particle size

The particle size plays a crucial role in the solubility of the samples. In general, smaller sizes enhance solubility, justified by an increased surface area (Joy et al., 2020; Tran et al., 2019). Fig. 1 illustrates the distributions in volume (with the respective $d_{4,3}$ and span values) and in number for all produced samples.

All samples showed a multimodal distribution in volume (Fig. 1A) with quite similar profiles, except for the CPS-pH sample, whose distribution was displaced to larger sizes. This was reflected in the higher

Table 2

Colour parameters (L^* , a^* , b^* , and the ΔE values) and the corresponding RGB colour of the SDs prepared under controlled pH conditions (pH = 6).

| Sample | L^* | a^* | b^* | ΔE | RGB colour |
|---------|------------------|------------------|------------------|------------------|------------|
| CPVP-pH | 83.63 ± 0.03 | 3.52 ± 0.02 | 94.95 ± 0.06 | - | |
| CKC-pH | 82.96 ± 0.02 | 7.54 ± 7.54 | 80.42 ± 0.01 | 15.09 ± 0.06 | |
| CMD-pH | 72.31 ± 0.01 | 23.00 ± 0.02 | 85.59 ± 0.08 | 24.39 ± 0.06 | |
| CAG-pH | 75.03 ± 0.01 | 19.70 ± 0.02 | 86.92 ± 0.06 | 20.01 ± 0.02 | |
| CPS-pH | 77.85 ± 0.04 | 15.42 ± 0.38 | 92.25 ± 0.26 | 13.50 ± 0.34 | |
| CPC-pH | 76.35 ± 0.08 | 17.85 ± 0.09 | 78.96 ± 0.08 | 22.67 ± 0.11 | |

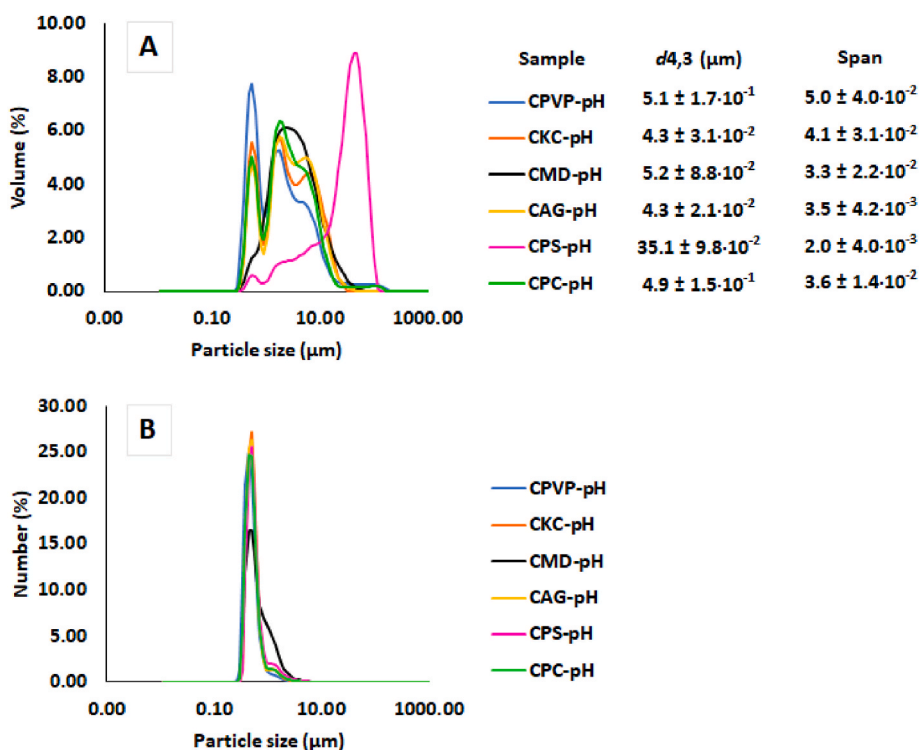


Fig. 1. Particle size distributions: A) in volume with respective mean diameter ($d_{4,3}$) and span, and B) in number. Sample codes are according to Table 1.

$d_{4,3}$ value ($35.1 \mu\text{m}$) compared to the others that fall within the 4.3 – $5.2 \mu\text{m}$ range. The observed effect can be related to the used polymer, PS, which can undergo a partial gelatinisation during the SD preparation, resulting in larger particle sizes (Tako and Hizukuri, 2002). In fact, at moderate temperatures (40 – $65 \text{ }^\circ\text{C}$), the starch granules can swell due to the water absorbed at the amorphous regions, inducing amylose release and retaining the water within the amylopectin double helixes structure (Bertoft and Blennow, 2016; Singh et al., 2016). Different factors, including the granule size and the amylose/amylopectin ratio, can hinder a simultaneous swelling of all granules, resulting in a partial gelatinisation (Ratnayake and Jackson, 2007), as can be expected in the SD production due to the applied slight heat. These larger granules impacted the volume distribution but not the number distribution, which is in the same range as other produced samples. The span values ranged from 2.0 (CPS-pH) to 5.0 (CPVP-pH).

In number, all formulations led to similar narrow and unimodal distribution profiles (Fig. 1B), centred in a particle size around $0.5 \mu\text{m}$ (D50). Similar results were found in the literature, i.e., circa $0.45 \mu\text{m}$, according to Li et al. (2015) for curcumin-Eudragit® E PO SDs. In the

case of volume distribution, the presence of a few bulky particles led to a larger mean particle size. Nevertheless, considering the number distribution, the particles are primarily of small size, endorsing an essential aspect of the SDs formulations.

3.3. FTIR analysis

The FTIR analysis of the SDs can help to perceive the development of polymer-curcumin hydrogen bonding leading to curcumin crystallinity modification (Lan et al., 2019; Nogami et al., 2021; Zong et al., 2022). The higher the extension of this phenomenon, the higher the impact on crystallinity reduction and, thus, on water compatibility enhancement. The polymer-curcumin hydrogen bonding can also help stabilise SDs, preventing curcumin recrystallisation and retaining solubility characteristics over time. PMs of the same composition were also analysed to better disclose the interactions since they are not expected to occur when the compounds are just mixed. In Fig. 2A–F, the spectra of curcumin, polymer, SD (with pH control) and the corresponding PM are presented.

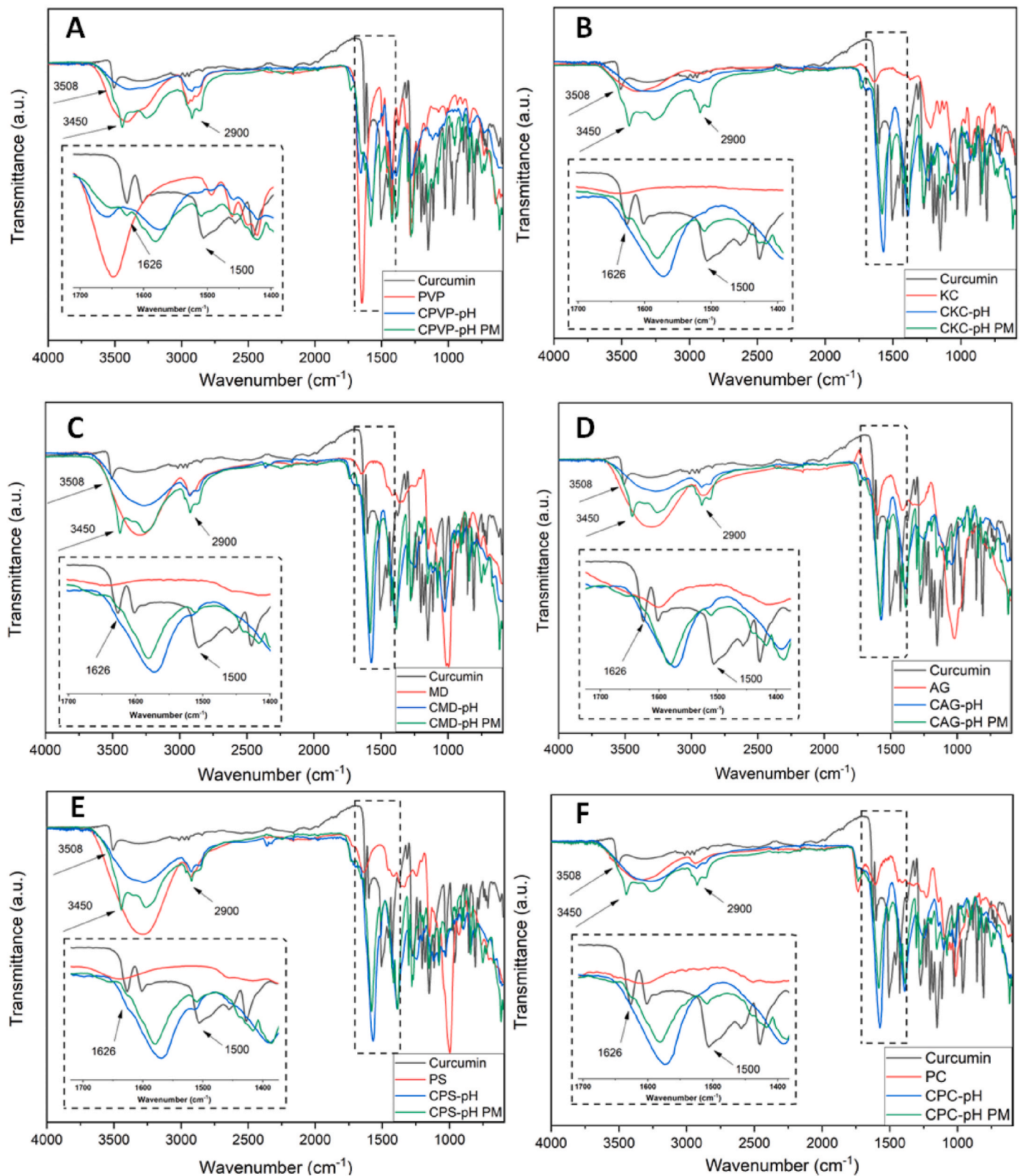


Fig. 2. FTIR spectra of the solid dispersions and corresponding physical mixtures (PMs) according to the used polymer: A. Polyvinylpyrrolidone (PVP), B. k-carrageenan (KC), C. Maltodextrin (MD), D. Arabic gum (AG), E. Potato starch (PS) and F. Pectin (PC). For comparison purposes, curcumin spectrum was added. Sample codes are according to [Table 1](#). When PM is added, it refers to the corresponding physical mixture. Arrows are used to assign the most representative FTIR vibrations.

In the curcumin spectrum, the peak at 3508 cm^{-1} corresponds to the OH stretching vibration, while at 1626 cm^{-1} , C=C and C=O overlapping vibrations are observed, assigned to a keto-enol tautomer (Wegiel et al., 2014). The vibration at 1601 cm^{-1} is associated with the symmetric stretching vibrations of aromatic rings (C=C). The vibration at 1507 cm^{-1} is assigned to the mixed vibrations of C=O and C-C=O groups, characteristic of the β -diketone group, while the C-O peak of the enol group is identified at 1272 cm^{-1} . The C-O-C vibration is detected at 1025 cm^{-1} (Ismail et al., 2014).

Considering the FTIR spectra for all PMs, specific vibrations were identified according to the contributions of the used polymer. The sharp stretching vibration peak detected at 3450 cm^{-1} is related mainly to the OH groups of curcumin, while the vibration at 3200 cm^{-1} is associated with the overlapped polymer and salts OH groups. In addition, the polymer and curcumin C-H stretching vibrations are detected at 2900 cm^{-1} , while the peak at 1500 cm^{-1} is assigned to the curcumin C=O and C-C=O groups. The peak detected at 1580 cm^{-1} is related to the C=O asymmetric stretching of the COO- group, attributed to the presence of salts in the formulations. In summary, PM spectra presented the influence of the individual components, corroborating the absence or the presence of weak polymer-curcumin molecular interactions.

For SDs, the OH stretching vibration of curcumin (3508 cm^{-1}) disappeared, and a remarkable broadening of the OH peak ($3300 - 3200\text{ cm}^{-1}$) occurred. This relates to the developed polymer-curcumin hydrogen bonding in SD formulations (Dharmalingam et al., 2021). Wegiel et al. (2014) found a similar behaviour in their study with curcumin-PVP SDs, suggesting also the peak shift to lower wavenumber values.

Curcumin is reported to form hydrogen bonds with the solubilizing carriers through phenolic hydroxyl, methoxy, or enol groups (He et al., 2019). In accordance, the curcumin C=O peak identified at 1507 cm^{-1} almost disappeared in all SD formulations, supporting the effective curcumin entrapment inside the polymer matrix. Additionally, the spectra of PMs present a shoulder at approximately 1626 cm^{-1} (carbonyl region) for all the samples, while for SDs this shoulder disappeared or shifted to lower wavenumber values. This change agrees with the curcumin-polymer hydrogen bonding formation (Wegiel et al., 2014).

3.4. DSC analysis

DSC is typically used with SDs to evaluate the melting temperature modifications of the active compound when it changes from a crystalline to an amorphous structure (Kumar and Kumar, 2021). The curcumin SDs (with and without pH control) and the PMs were analysed by DSC, and the thermograms are shown in Fig. 3. The samples produced without pH control were considered to analyse salt's effect on curcumin crystallinity.

The endothermic peak at $181.8\text{ }^\circ\text{C}$, observed in the curcumin thermogram, is typical of the curcumin's most stable crystalline polymorphism, form 1 (Sanphui et al., 2011). The citric acid and sodium citrate (supplementary material - Fig. S1) show endothermic peaks at 161.5 and $167.6\text{ }^\circ\text{C}$, respectively. The endothermic peaks observed at 214 and $318\text{ }^\circ\text{C}$ for citric acid and sodium citrate, respectively, were related to their thermal degradation (Gao et al., 2012; Klímová and Leitner, 2012).

All the PMs presented the same thermogram patterns, with an endothermic peak between 165 and $169\text{ }^\circ\text{C}$, coincident with the crystalline salts peaks. In the PMs, curcumin melting temperature can decrease due to a purity drop resulting from the mixture with other compounds (Mai et al., 2020). In accordance, in PMs, curcumin melting temperature can decrease, overlapping with the salt peaks. Additionally, low curcumin contents in the formulations can make it difficult to identify the curcumin peak. Besides, all the samples showed endothermic peaks between 324 and $330\text{ }^\circ\text{C}$, characteristic of the sodium citrate ($318.7\text{ }^\circ\text{C}$), considering the amount of this salt in the formulations.

SDs produced with pH control presented an endothermic peak located between 190 and $197\text{ }^\circ\text{C}$, related to the presence of curcumin. An exception was the CKC-pH system, which showed a peak at $177\text{ }^\circ\text{C}$, related to curcumin. Moreover, an endothermic peak at $189\text{ }^\circ\text{C}$, a characteristic melting peak for PC, was observed for the CPC-pH sample. This shift is due to the change in the curcumin crystallinity during the SD process, where the crystalline form 1 is transformed into crystalline form 2, giving rise to an endothermic peak at lower temperatures, in accordance with Pandey and co-workers in a study addressing the study of curcumin polymorphs thermal behaviour (Pandey and Dalvi, 2019; Sanphui et al., 2011).

The analysis of the reference formulations, i.e., those prepared without pH control, removed the influence of salts and thus the overlapping with curcumin melting peaks. These systems generally presented lower melting temperatures (T_m), 175 to $178\text{ }^\circ\text{C}$, or no curcumin melting peak, except for CKC-Ref, for which a T_m around $180\text{ }^\circ\text{C}$ is observed. This behaviour can be associated with curcumin transformation into a less crystalline system and, possibly, a less stable polymorph, reflected by lower T_m (Pandey and Dalvi, 2019). Although most of the existing literature addresses that an ideal amorphous SD system is distinguished by the complete absence of a melting peak, certain compounds, such as curcumin, can undergo partial amorphisation, also impacting solubility.

3.5. XRD analysis

The produced samples were subjected to XRD analysis. Fig. 4 shows the diffractograms of the curcumin, SDs with and without pH control, and respective PMs. Regarding curcumin, a crystalline pattern typical of the crystalline form 1, also named the monoclinic form of curcumin, is observed, reflected in prominent peaks at 2θ to 12.19 , 14.49 , 17.25 , 18.17 , 23.29 , 23.68 , 24.60 and 25.59 , in agreement with the results found by Dharmalingam et al. (2021). Analysing the SDs crystalline patterns is relevant considering that the formed curcumin polymorphs directly affect stability and solubility (Suresh and Nangia, 2018). Polymorphism occurs due to changes in the crystalline structure caused by molecular conformation, interactions, or crystal packing modifications. Many works dealing with the solubility of different curcumin polymorphs suggested that variations in the polymorphism can allow the improvement of solubility up to 4 times, in some cases, up to 25 times when compared to the most stable solid crystalline phase (form 1). It is consensual that form 3 is less stable than form 2 and form 1. The solubility order is form 3 > form 2 > form 1 (Pandey and Dalvi, 2019; Sanphui and Bolla, 2018). In SDs, by decreasing curcumin crystallinity, a water solubility enhancement is achieved. By changing from a crystalline state to an amorphous or partially amorphous state, curcumin's crystal lattice structure is disrupted, weakening curcumin intermolecular forces. This increases curcumin surface area and reduces aggregation, allowing curcumin molecules to better interact with the water molecules.

The polymers generally show amorphous patterns, except PS, which presented a semi-crystalline form (supplementary material - Fig. S2). The PM patterns showed the peaks of the base curcumin, possibly due to the weak or in-existent polymer-curcumin molecular interactions.

In general, all the SD samples presented diffractograms with few peaks, indicating a significant reduction in the curcumin crystalline domains. Concerning the SDs, while some polymers favoured curcumin crystalline structure modification for controlled pH conditions, for others, this modification is more evident without controlled pH. Particularising for most of the studied polymers, namely PVP, MD, AG, and PS, natural pH (i.e., a pH in the range of 4–5) is effective in achieving curcumin amorphisation, i.e., in favouring hydrogen bonding between curcumin and the polymer. For KC and PC, a controlled pH of 6.0 resulted in a better effect. These two polymers hold gel formation capacity, which is hindered at pH 6 due to salt addition, keeping the availability of functional groups to participate in hydrogen bonding with

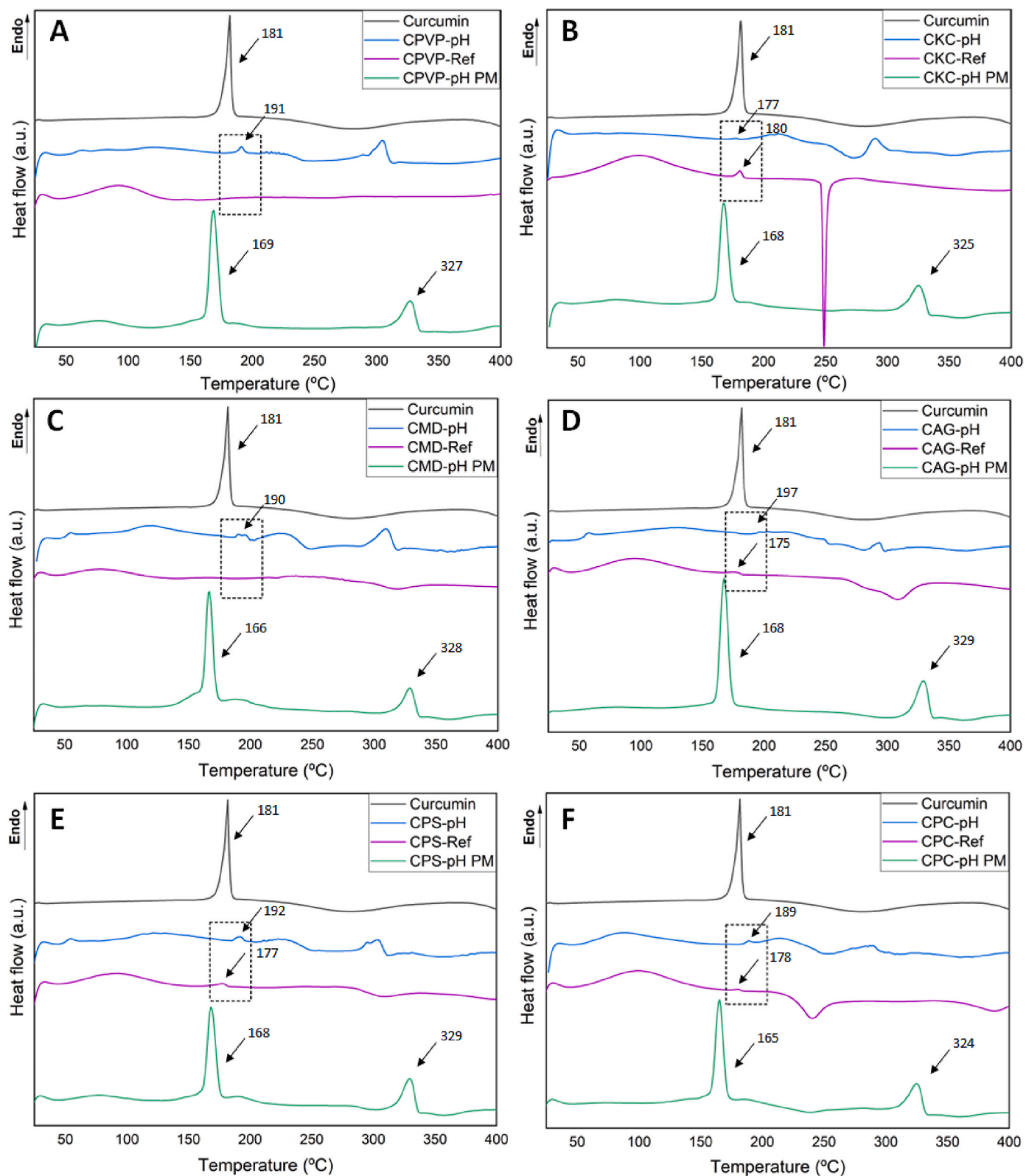


Fig. 3. DSC thermograms of the solid dispersions and corresponding physical mixtures (PMs) according to the used polymer: A. Polyvinylpyrrolidone (PVP), B. k-carrageenan (KC), C. Maltodextrin (MD), D. Arabic gum (AG), E. Potato starch (PS) and F. Pectin (PC). For comparison purposes, curcumin thermogram was added. Sample codes are according to Table 1. When PM is added, it refers to the corresponding physical mixture. The dashed rectangle highlights the principal endothermic peaks in the SDs formulations (pH and references).

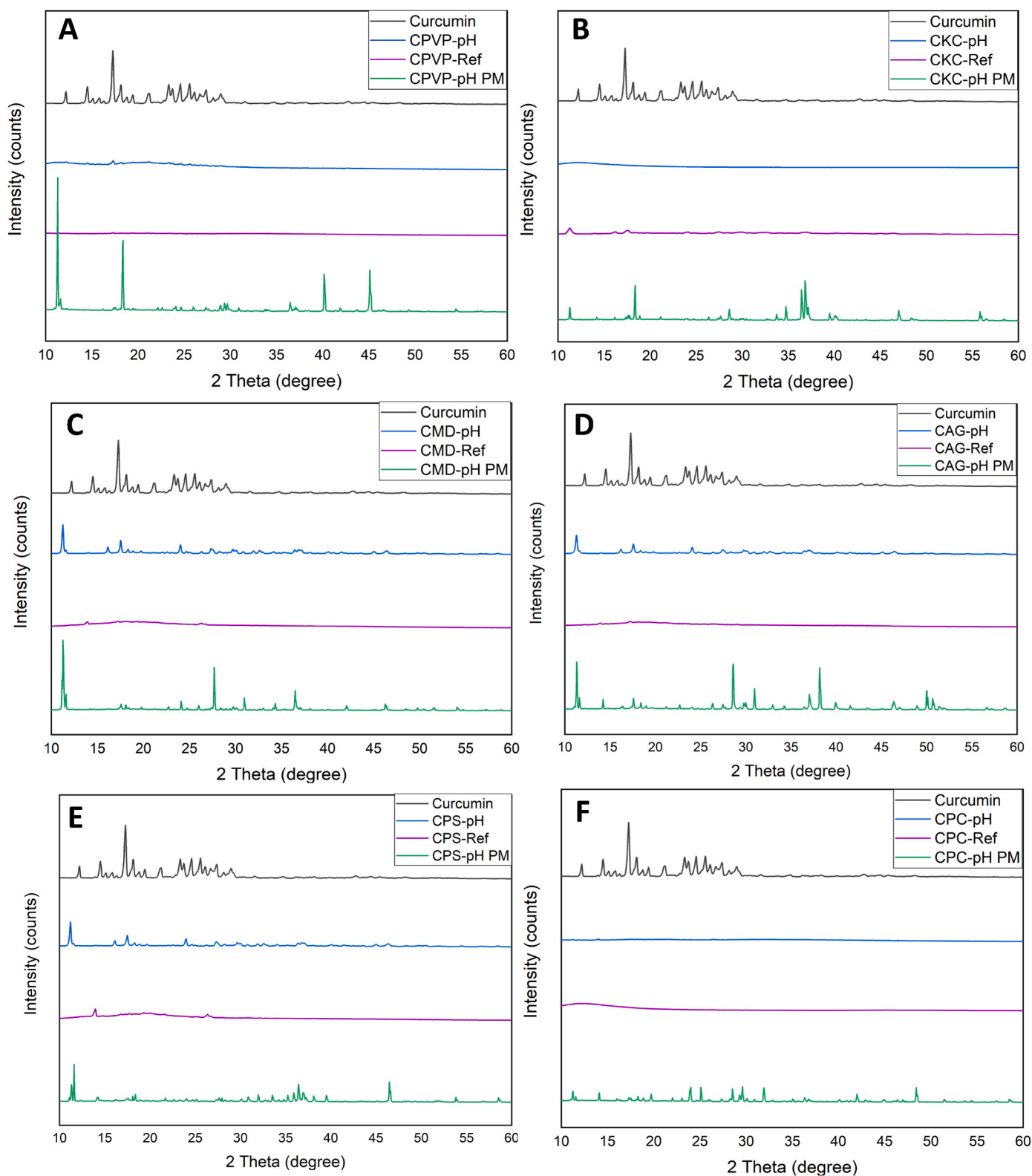


Fig. 4. XRD analysis of solid dispersions and corresponding physical mixtures (PMs) according to the used polymer: A. Polyvinylpyrrolidone (PVP), B. k-carrageenan (KC), C. Maltodextrin (MD), D. Arabic gum (AG), E. Potato starch (PS) and F. Pectin (PC). For comparison purposes, curcumin thermogram was added. Sample codes are according to [Table 1](#). When PM is added, it refers to the corresponding physical mixture.

curcumin. This behaviour was corroborated by the DSC results, where most systems produced without pH control (CPVP-Ref, CMD-Ref, CAG-Ref and CPS-Ref) presented patterns compatible with lower-ordered structures. Regarding the XRD results, the polymorph pattern change

is perceptible mainly in CMD-Ref, CAG-Ref and CPS-Ref samples ([Fig. 4C–E](#)). When produced at pH 6 (controlled pH), the samples revealed a higher degree of crystallinity. In general, the sharp peaks were drastically reduced for the samples without pH control, indicating

a higher amorphisation in these systems, with just a small influence of crystallinity observed at 14 20. These patterns suggest that curcumin is mostly amorphous, with just some crystalline parts.

3.6. Solubility tests

Table 3 presents the water solubility of SDs produced with and without pH control and respective PMs for 24 h. The formulations without pH control were assessed to verify the influence of the salts on the solubility. According to the literature, the solubility of curcumin in water is reported to be in the order of 0.03–4 µg/mL at temperatures between 30 and 37 °C, depending on the purity, brand, and other factors (Mai et al., 2020; Moideen et al., 2020; Teixeira et al., 2016). The low curcumin solubility (<1 µg/mL) was corroborated in the present work, as the measured absorbance of curcumin-saturated solutions was below the detection limit.

As can be seen in Table 3, the curcumin solubility values for the PMs were very similar, with no statistically significant differences, between 7 and 8 µg/mL, thus at least 7–8 times higher than the apparent solubility of the free curcumin. Other authors have also reported a significant increase in the curcumin solubility in the PMs compared to untreated curcumin (Teixeira et al., 2016). The favourable molecular interactions of the polymer and/or salts with curcumin in the aqueous solutions can justify this behaviour. The curcumin solubility for all PMs decreased (2–5 %) between 2 and 24 h, though statistical analysis showed these differences were not significant ($\alpha = 0.05$, supplementary material - Table S1). In fact, this behaviour was expected since curcumin was not mixed at the molecular level, which is the case in SDs.

Regarding the SDs, the solubility of the formulations produced with pH control varied between 25 and 37 µg/mL. In contrast, the reference systems (SDs without pH control) ranged from 18 to 86 µg/mL at 24 h, when compared to pristine curcumin (Table 3). Comparing the SDs with the PMs, SDs promoted a higher curcumin solubility enhancement. Higher values can be found in the literature, most often using very effective pharmaceutical carriers like solutol® HS15120, for which 550 times enhancement was observed (Seo et al., 2012). Increases of 120–150 times were observed when using skimmed milk powder but with solubilities measured at 37 °C (Moideen et al., 2020). Lower increments were observed when using PVP (12 times) with solubilities measured at 25 °C (He et al., 2019), and circa 4 times using cellulose acetate added with 10 % mannitol, measured at 25 °C using an ethanolic mixture as the solubilizing medium (Wan et al., 2012).

In the SDs with pH control, there was a significant decrease in the solubility (3–15 %) between 2 and 24 h, except for the CKC samples, which remained unchanged. The CMD samples showed the highest solubility, which increased by 8 % from 2 to 24 h. For the other reference samples, the decrease in solubility varied from 2 to 19 %, though the differences were not statistically significant (Table S1). In the case of SDs with pH control, there are no significant differences between most of the samples (CPVP-pH, CMD-pH, CAG-pH and CPS-pH), except for CKC-pH

Table 3

Solubility in water (µg/mL, at 25 °C, measured after 2 and 24 h) of physical mixtures and solid dispersions reflecting the selected polymer and used pH conditions (with pH control (pH = 6) and without pH control (natural pH)).

| Polymer | Physical mixtures | Solid dispersions | |
|----------------------|--------------------------|---------------------------|---------------------------|
| | | With pH control | Without pH control |
| Polyvinylpyrrolidone | 7.70 ± 0.49 ^a | 24.54 ± 0.57 ^c | 28.34 ± 0.61 ^c |
| K-carrageenan | 7.53 ± 0.60 ^a | 29.71 ± 1.25 ^b | 19.67 ± 2.29 ^d |
| Maltodextrin | 7.93 ± 0.31 ^a | 26.67 ± 1.22 ^c | 86.23 ± 1.68 ^a |
| Arabic gum | 7.79 ± 0.26 ^a | 25.39 ± 0.96 ^c | 27.93 ± 1.60 ^c |
| Potato starch | 7.66 ± 0.31 ^a | 25.26 ± 0.35 ^c | 40.43 ± 2.11 ^b |
| Pectin | 7.68 ± 0.21 ^a | 36.54 ± 0.58 ^a | 18.10 ± 2.14 ^d |

Results are presented as mean ± standard deviation. Different letters in each column correspond to significant differences ($\alpha = 0.05$).

and CPC-pH. Contrarily, the reference systems (without pH control) presented significant differences among samples but with a similarity between CPVP-Ref and CAG-Ref, and CKC-Ref and CPC-Ref (Table 3).

The relationship between the solubility and the curcumin-polymer molecular interactions is inherent. Some authors associated the increase of these interactions, especially hydrogen bonds, with decreased curcumin crystallinity and, thus, solubility increase. Xi and co-workers observed a significant enhancement in the curcumin solubility when the SDs were produced with Kollidon CLSF and surfactant TPGS, attributing this improvement to the strong hydrogen bonding between the polymer and curcumin and the effect of the surfactant (Xi et al., 2023). In another recent work addressing SDs applied to curcumin with hydroxypropyl-β-cyclodextrin, the solubility of the SDs varied between 0.27 and 14.16 µg/mL, at 30 °C, much higher than the solubility of curcumin in water (0.03 µg/mL), also reported by the authors (Mai et al., 2020).

Curcumin is known to be stable in acidic conditions (pH from 3.0 to 6.5), with pH impacting the polymer-curcumin molecular interactions. Generally, SDs produced without pH control presented lower pH values, and enhanced solubility was observed compared to their counterparts produced with pH control. Except for the CAG samples, all the formulations with and without pH control presented significant solubility differences.

In general, adding salts to control the pH influences the interactions between curcumin and the polymer, affecting curcumin crystallinity and, thus, solubility. This effect is generally ruled by the type of functional groups in the polymer molecules and their capacity to participate in hydrogen bonding with curcumin. Nevertheless, competing phenomena like gel formation can interfere with this process. This is the case of PC and KC. In the case of PC, gel formation is promoted for low pHs (2.5–3.5), which can be observed for the CPC-Ref sample (natural pH of 3.17). This effect is due to the intensification of hydrophobic forces (interactions involving methyl ester groups) and hydrogen bonding (interactions involving carboxyl and secondary alcohol groups) (Said et al., 2023). In such conditions, the polymer-curcumin interactions are hindered. For pH 6, gel formation does not occur due to salt addition, keeping the functional groups of the polymer available to participate in hydrogen bonding with curcumin, favouring curcumin amorphisation and, thus, solubility. In what concerns KC, where similar pHs are observed, 6.0 and 6.18, respectively, for medium with and without pH control, the presence of Na⁺ ions, due to sodium citrate addition, hinders the gelation process (Tako, 2015), resulting in a similar effect to the one previously described for PC.

The partial gelatinisation process occurring during the starch-based SDs preparation would not facilitate the formation of a structural network as in the case of KC and PC, maintaining a behaviour similar to the rest of the studied formulations.

4. Conclusions

In this work, natural-based SDs based on k-carrageenan (KC), maltodextrin (MD), Arabic gum (AG), potato starch (PS), and pectin (PC) were evaluated against the synthetic benchmark polyvinylpyrrolidone (PVP). The objective was to obtain curcumin-based water-dispersible colourant formulations, a need for the food industry urging for natural and less toxic alternatives, particularly in the red and yellow shades.

The observed colour was polymer-dependent, with the SDs based on MD, AG, and PC presenting a deeper orange colouration than PVP, which resembles KC- and PS-based SDs. Similar size distributions were achieved in volume and number for all formulations except PS-based SDs, whose volume distribution shifted to higher values. During SDs formation, polymer-curcumin hydrogen bonding intensifies, as confirmed by FTIR. This impacted curcumin crystallinity, as observed by DSC and XRD analysis. Lower curcumin melting temperatures were registered for MD-, AG-, and PS-based SDs without pH control. This

effect was more pronounced for the KC-based SD produced at pH 6. XRD corroborated curcumin crystallinity reduction, which impacted water solubility.

A significant increase in curcumin solubility was obtained using SDs. PS- and MD-based SDs produced at natural pH, had a noteworthy water solubility increase, 40.43 and 86.28 µg/mL, respectively, higher than PVP-based SDs (28.34 µg/mL). For SDs produced at pH 6, all SDs based on natural polymers resulted in increased water solubility comparatively to PVP (24.54 µg/mL), e.g., KC and PC-based SDs with values of 29.71 and 36.54 µg/mL, respectively. The corresponding PMs presented considerably lower solubility, corroborating the impact of the SDs technology on curcumin amorphisation and solubility increase.

Even though using natural pH, most of the used polymers gave rise to SDs presenting increased water solubility, pH control (pH 6) made possible a standardised method less dependent on the used polymer, which is relevant from an industrial point of view.

CRedit authorship contribution statement

Stephany Cunha de Rezende: Writing – original draft, Methodology, Investigation, Conceptualization. **Olga Ferreira:** Writing – review & editing, Methodology, Investigation. **Arantzazu Santamaria-Echart:** Writing – review & editing, Supervision, Conceptualization. **Madalena Maria Dias:** Writing – review & editing, Supervision. **Maria Filomena Barreiro:** Writing – review & editing, Supervision, Resources, Funding acquisition, Conceptualization.

Declaration of competing interest

The authors declare that they have no known competing financial interests or personal relationships that could have appeared to influence the work reported in this paper.

Data availability

No data was used for the research described in the article.

Acknowledgements

The authors are grateful to the Foundation for Science and Technology (FCT, Portugal) and FEDER under Programme PT2020 for financial support to CIMO (UIDB/00690/2020 and UIDP/00690/2020) and SusTEC (LA/P/0007/2021), LSRE-LCM (UIDB/50020/2020 and UIDP/00690/2020) and ALiCE (LA/P/0045/2020). FCT for the Research grant SFRH/BD/147326/2019 of Stephany C. de Rezende and national funding by FCT, PI, through the institutional scientific employment program contract for Arantzazu Santamaria-Echart. In addition, the technical support provided by I3Bs- Research Institute on Biomaterials, Biodegradables and Biomimetics of the University of Minho is also acknowledged.

Appendix A. Supplementary data

Supplementary data to this article can be found online at <https://doi.org/10.1016/j.jfoodeng.2024.111986>.

References

- Balakrishnan, M., Gayathiri, S., Preetha, P., Pandiselvam, R., Jeevarathinam, G., 2021. Microencapsulation of bixin pigment by spray drying : evaluation of characteristics. *LWT-Food Sci. Technol.* 145, 111343 <https://doi.org/10.1016/j.lwt.2021.111343>.
- Bertoft, E., Blennow, A., 2016. Structure of potato starch. In: *Advances in Potato Chemistry and Technology*. Elsevier Inc., pp. 57–73. <https://doi.org/10.1016/B978-0-12-800002-1.00003-0>
- Boer, F.Y. De, Imhof, A., Velikov, K.P., 2019. Encapsulation of colorants by natural polymers for food applications. *Coloration Technol.* 135, 183–194. <https://doi.org/10.1111/cote.12393>.
- Christina, B., Taylor, L.S., Mauer, L.J., 2015. Physical stability of L-ascorbic acid amorphous solid dispersions in different polymers: a study of polymer crystallization inhibitor properties. *Food Res. Int.* 76, 867–877. <https://doi.org/10.1016/j.foodres.2015.08.009>.
- Dharmalingam, K., Anandalakshmi, R., Shekhar, S., 2021. Microwave-induced diffusion method for solid dispersion of curcumin in HPMC matrix using water as hydration carrier. *J. Dispersion Sci. Technol.* 42, 1419–1430. <https://doi.org/10.1080/01932691.2020.1770608>.
- Faisal, W., Ruane-O'Hora, T., O'Driscoll, C.M., Griffin, B.T., 2013. A novel lipid-based solid dispersion for enhancing oral bioavailability of Lycopene - in vivo evaluation using a pig model. *Int. J. Pharm.* 453, 307–314. <https://doi.org/10.1016/j.ijpharm.2013.06.027>.
- Fernández-López, J.A.J.A., Fernández-Lledó, V., Angosto, J.M.J.M., 2020. New insights into red plant pigments: more than just natural colorants. *RSC Adv.* 10, 24669–24682. <https://doi.org/10.1039/D0RA03514A>.
- Gao, J., Wang, Y., Hao, H., 2012. Investigations on dehydration processes of trisodium citrate hydrates. *Front. Chem. Sci. Eng.* 6, 276–281. <https://doi.org/10.1007/s11705-012-1206-4>.
- Gordillo, B., Sigurdson, G.T., Lao, F., González-Miret, M.L., Heredia, F.J., Giusti, M.M., 2018. Assessment of the color modulation and stability of naturally copigmented anthocyanin-grape colorants with different levels of purification. *Food Res. Int.* 106, 791–799. <https://doi.org/10.1016/j.foodres.2018.01.057>.
- He, Y., Liu, H., Bian, W., Liu, Y., Liu, X., Ma, S., Zheng, X., Du, Z., Zhang, K., Ouyang, D., 2019. Molecular interactions for the curcumin-polymer complex with enhanced anti-inflammatory effects. *Pharmaceutics* 11, 1–21. <https://doi.org/10.3390/pharmaceutics11090442>.
- Ishimoto, K., Miki, S., Ohno, A., Nakamura, Y., Otani, S., Nakamura, M., Nakagawa, S., 2019. β -Carotene solid dispersion prepared by hot-melt technology improves its solubility in water. *J. Food Sci. Technol.* 56, 3540–3546. <https://doi.org/10.1007/s13197-019-03793-8>.
- Ismail, E.H., Sabry, D.Y., Mahdy, H., Khalil, M.M.H., 2014. Synthesis and characterization of some ternary metal complexes of curcumin with 1,10-phenanthroline and their anticancer applications. *J. Sci. Res.* 6, 509–519. <https://doi.org/10.3329/jsr.v6i3.18750>.
- Joy, S.A., Raju, T., Lal Prasanth, M.L., Prasanth, S., 2020. Tool to increase solubility: solid dispersion. *J. Pharmaceut. Sci. Res.* 12, 1220–1226.
- Karma, I.G.M., 2020. Determination and measurement of color Dissimilarity. *Int. J. Eng. Emerg. Technol.* 5, 67–71.
- Khan, K.U., Minhas, M.U., Badshah, S.F., Suhail, M., Ahmad, A., Ijaz, S., 2022. Overview of nanoparticulate strategies for solubility enhancement of poorly soluble drugs. *Life Sci.* 291, 120301 <https://doi.org/10.1016/j.lfs.2022.120301>.
- Klímová, K., Leitner, J., 2012. DSC study and phase diagrams calculation of binary systems of paracetamol. *Thermochim. Acta* 550, 59–64. <https://doi.org/10.1016/j.tca.2012.09.024>.
- Kumar, A., Kumar, J., 2021. Solid dispersion techniques: a review. *Int. J. Res. Eng. Sci. Manag.* 4, 104–111.
- Lan, Y., Xu, M., Ohm, J.B., Chen, B., Rao, J., 2019. Solid dispersion-based spray-drying improves solubility and mitigates beany flavour of pea protein isolate. *Food Chem.* 278, 665–673. <https://doi.org/10.1016/j.foodchem.2018.11.074>.
- Leimann, V.F., Gonçalves, O.H., Sorita, G.D., Rezende, S., Bona, E., Fernandes, I.P.M., Ferreira, I.C.F.R., Barreiro, M.F., 2019. Heat and pH stable curcumin-based hydrophilic colorants obtained by the solid dispersion technology assisted by spray-drying. *Chem. Eng. Sci.* 205, 248–258. <https://doi.org/10.1016/j.ces.2019.04.044>.
- Li, J., Lee, I.W., Shin, G.H., Chen, X., Park, H.J., 2015. Curcumin-Eudragit® e PO solid dispersion: a simple and potent method to solve the problems of curcumin. *Eur. J. Pharm. Biopharm.* 94, 322–332. <https://doi.org/10.1016/j.ejpb.2015.06.002>.
- Lin, Q., Wu, D., Singh, H., Ye, A., 2021. Improving solubility and stability of β -carotene by microencapsulation in soluble complexes formed with whey protein and OSA-modified starch. *Food Chem.* 352, 1–9. <https://doi.org/10.1016/j.foodchem.2021.129267>.
- Mai, N.N.S., Nakai, R., Kawano, Y., Hanawa, T., 2020. Enhancing the solubility of curcumin using a solid dispersion system with hydroxypropyl- β -cyclodextrin prepared by Grinding, freeze-drying, and common solvent evaporation methods. *J. Pharm. (Lahore)* 8, 1–14.
- Medeiros, A.K.O.C., Gomes, C.C., Amaral, M.L.Q.A., Medeiros, L.D.G., Medeiros, I., Porto, D.L., Aragão, C.F.S., Maciel, B.L.L., Morais, A.H.A., Passos, T.S., 2019. Nanoencapsulation improved water solubility and color stability of carotenoids extracted from Cantaloupe melon (*Cucumis melo* L.). *Food Chem.* 270, 562–572. <https://doi.org/10.1016/j.foodchem.2018.07.099>.
- Meliana, Y., Utami, D., Septiyanti, M., Wulandari, E.T., Ghazali, M., Restu, W.K., Fahmiati, S., Lelono, R.A.A., 2020. Characterization of artemisinin solid dispersion in maltodextrin and gum Arabic by freeze dried and high energy milling methods. *Macromol. Symp.* 391, 1900186 <https://doi.org/10.1002/masy.201900186>.
- Meng, F., Trivino, A., Prasad, D., Chauhan, H., 2015. Investigation and correlation of drug polymer miscibility and molecular interactions by various approaches for the preparation of amorphous solid dispersions. *Eur. J. Pharmaceut. Sci.* 71, 12–24. <https://doi.org/10.1016/j.ejps.2015.02.003>.
- Mezquita, P.C., Álvarez, C.E., Ramírez, J.P., Muñoz, W.B., Fuentes, F.S., Ruiz-Domínguez, M.D.C., 2020. Isotonic beverage pigmented with water-dispersible emulsion from astaxanthin oleoresin. *Molecules* 25, 1–16. <https://doi.org/10.3390/molecules25040841>.
- Moideen, M.M.J., Alqahtani, A., Venkatesan, K., Ahmad, F., Krisharaju, K., Gayasuddin, M., Shaik, R.A., Ibraheem, K.M.M., Salama, M.E., dosoky, M., Abed, S. Y., 2020. Application of the Box-Behnken design for the production of soluble curcumin: skimmed milk powder inclusion complex for improving the treatment of

- colorectal cancer. *Food Sci. Nutr.* 8, 6643–6659. <https://doi.org/10.1002/fsn3.1957>.
- Nadaf, S., Jadhav, A., Killedar, S., 2021. Mung bean (*Vigna radiata*) porous starch for solubility and dissolution enhancement of poorly soluble drug by solid dispersion. *Int. J. Biol. Macromol.* 167, 345–357. <https://doi.org/10.1016/j.ijbiomac.2020.11.172>.
- Nogami, S., Minoura, K., Kiminami, N., Kitaura, Y., Uchiyama, H., Kadota, K., Tozuka, Y., 2021. Stabilizing effect of the cyclodextrins additive to spray-dried particles of curcumin/polyvinylpyrrolidone on the supersaturated state of curcumin. *Adv. Powder Technol.* 32, 1750–1756. <https://doi.org/10.1016/j.apt.2021.03.032>.
- Otani, S., Miki, S., Nakamura, Y., Ishimoto, K., Ago, Y., Nakagawa, S., 2020. Improved bioavailability of β -carotene by amorphous solid dispersion technology in rats. *J. Nutr. Sci. Vitaminol.* 66, 207–210. <https://doi.org/10.3177/jnsv.66.207>.
- Pandey, K.U., Dalvi, S.V., 2019. Understanding stability relationships among three curcumin polymorphs. *Adv. Powder Technol.* 30, 266–276. <https://doi.org/10.1016/j.apt.2018.11.002>.
- Pandi, P., Bulusu, R., Kommineni, N., Khan, W., Singh, M., 2020. Amorphous solid dispersions: an update for preparation, characterization, mechanism on bioavailability, stability, regulatory considerations and marketed products. *Int. J. Pharm.* 586, 119560 <https://doi.org/10.1016/j.ijpharm.2020.119560>.
- Pinlaor, S., Jantawong, C., Intuyod, K., Sirijindalert, T., Pinlaor, P., Pairojkul, C., Charoensuk, L., Sitthirach, C., Vaeteewoottacharn, K., Puthongking, P., Priprem, A., 2021. Solid dispersion improves release of curcumin from nanoparticles: potential benefit for intestinal absorption. *Mater. Today Commun.* 26, 101999 <https://doi.org/10.1016/j.mtcomm.2020.101999>.
- Qi, W., Zhang, Z., Wu, T., 2020. Encapsulation of β -carotene in oleogel-in-water Pickering emulsion with improved stability and bioaccessibility. *Int. J. Biol. Macromol.* 164, 1432–1442. <https://doi.org/10.1016/j.ijbiomac.2020.07.227>.
- Ratnayake, W.S., Jackson, D.S., 2007. A new insight into the gelatinization process of native starches. *Carbohydr. Polym.* 67, 511–529. <https://doi.org/10.1016/j.carbpol.2006.06.025>.
- Said, N.S., Olawuyi, I.F., Lee, W.Y., 2023. Pectin Hydrogels: gel-Forming Behaviors, mechanisms, and food applications. *Gels* 9, 1–28. <https://doi.org/10.3390/gels9090732>.
- Sanphui, P., Bolla, G., 2018. Curcumin, a Biological Wonder molecule: a crystal Engineering point of view. *Cryst. Growth Des.* 18, 5690–5711. <https://doi.org/10.1021/acs.cgd.8b00646>.
- Sanphui, P., Goud, N.R., Khandavilli, U.B.R., Bhanoth, S., Nangia, A., 2011. New polymorphs of curcumin. *Chem. Commun.* 47, 5013–5015. <https://doi.org/10.1039/c1cc10204d>.
- Santos, D.T., Meireles, M.A., 2010. Carotenoid pigments encapsulation: Fundamentals, techniques and recent trends. *Open Chem. Eng. J.* 4, 42–50. <https://doi.org/10.2174/1874123101004020042>.
- Sato, Y., Joumura, T., Nashimoto, S., Yokoyama, S., Takekuma, Y., Yoshida, H., Sugawara, M., 2018. Enhancement of lymphatic transport of lutein by oral administration of a solid dispersion and a self-microemulsifying drug delivery system. *Eur. J. Pharm. Biopharm.* 127, 171–176. <https://doi.org/10.1016/j.ejpb.2018.02.013>.
- Seo, S.W., Han, H.K., Chun, M.K., Choi, H.K., 2012. Preparation and pharmacokinetic evaluation of curcumin solid dispersion using Solutol® HS15 as a carrier. *Int. J. Pharm.* 424, 18–25. <https://doi.org/10.1016/j.ijpharm.2011.12.051>.
- Singh, J., Colussi, R., McCarthy, O.J., Kaur, L., 2016. Potato starch and its modification. In: *Advances in Potato Chemistry and Technology*. Elsevier Inc., pp. 195–247. <https://doi.org/10.1016/B978-0-12-800002-1.00008-X>.
- Suresh, K., Nangia, A., 2018. Curcumin: pharmaceutical solids as a platform to improve solubility and bioavailability. *CrystEngComm* 20, 3277–3296. <https://doi.org/10.1039/c8ce00469b>.
- Tako, M., 2015. The principle of Polysaccharide gels. *Adv. Biosci. Biotechnol.* 6, 22–36. <https://doi.org/10.4236/abb.2015.61004>.
- Tako, M., Hizukuri, S., 2002. Gelatinization mechanism of potato starch. *Carbohydr. Polym.* 48, 397–401. [https://doi.org/10.1016/S0144-8617\(01\)00287-9](https://doi.org/10.1016/S0144-8617(01)00287-9).
- Teixeira, C.C.C., Mendonça, L.M., Bergamaschi, M.M., Queiroz, R.H.C., Souza, G.E.P., Antunes, L.M.G., Freitas, L.A.P., 2016. Microparticles containing curcumin solid dispersion: stability, bioavailability and anti-inflammatory activity. *AAPS PharmSciTech* 17, 252–261. <https://doi.org/10.1208/s12249-015-0337-6>.
- Tran, P., Pyo, Y.C., Kim, D.H., Lee, S.E., Kim, J.K., Park, J.S., 2019. Overview of the manufacturing methods of solid dispersion technology for improving the solubility of poorly water-soluble drugs and application to anticancer drugs. *Pharmaceutics* 11, 1–26. <https://doi.org/10.3390/pharmaceutics11030132>.
- Umemoto, Y., Uchida, S., Yoshida, T., Shimada, K., Kojima, H., Takagi, A., Tanaka, S., Kashiwagura, Y., Namiki, N., 2020. An effective polyvinyl alcohol for the solubilization of poorly water-soluble drugs in solid dispersion formulations. *J. Drug Deliv. Sci. Technol.* 55, 101401 <https://doi.org/10.1016/j.jddst.2019.101401>.
- Vo, C.L.N., Park, C., Lee, B.J., 2013. Current trends and future perspectives of solid dispersions containing poorly water-soluble drugs. *Eur. J. Pharm. Biopharm.* 85, 799–813. <https://doi.org/10.1016/j.ejpb.2013.09.007>.
- Wan, S., Sun, Y., Qi, X., Tan, F., 2012. Improved bioavailability of poorly water-soluble drug curcumin in cellulose acetate solid dispersion. *AAPS PharmSciTech* 13, 159–166. <https://doi.org/10.1208/s12249-011-9732-9>.
- Wegiel, L.A., Zhao, Y., Mauer, L.J., Edgar, K.J., Taylor, L.S., 2014. Curcumin amorphous solid dispersions: the influence of intra and intermolecular bonding on physical stability. *Pharmaceut. Dev. Technol.* 19, 976–986. <https://doi.org/10.3109/10837450.2013.846374>.
- Xi, Z., Fei, Y., Wang, Y., Lin, Q., Ke, Q., Feng, G., Xu, L., 2023. Solubility improvement of curcumin by crystallization inhibition from polymeric surfactants in amorphous solid dispersions. *J. Drug Deliv. Sci. Technol.* 83, 104351 <https://doi.org/10.1016/j.jddst.2023.104351>.
- Zhang, Q., Wang, H., Feng, Z., Lu, Z., Su, C., Zhao, Y., Yu, J., Dushkin, A.V., Su, W., 2021. Preparation of pectin-tannic acid coated core-shell nanoparticle for enhanced bioavailability and antihyperlipidemic activity of curcumin. *Food Hydrocolloids* 119, 106858. <https://doi.org/10.1016/j.foodhyd.2021.106858>.
- Zong, S., Liu, Y., Park, Hyun J., Ye, M., Li, J., Zong, S., Liu, Y., Park, Hyun Jin, Ye, M., J L, D., 2022. Curcumin solid dispersion based on three model acrylic polymers: formulation and release properties. *Brazilian J. Pharm. Sci.* 58, 1–14.